Title
HUMAN KIDNEY CELL OXYGEN-ENHANCEMENT RATIOS FOR FAST-NEUTRON BEAMS AND A PREDICTION FOR NEGATIVE PION BEAMS

Author
Curtis, Stanley B.

Publication Date
1970

Submitted to Radiation Research

UCRL-19456
Preprint

c. 2

HUMAN KIDNEY CELL OXYGEN-ENHANCEMENT RATIOS FOR FAST-NEUTRON BEAMS AND A PREDICTION FOR NEGATIVE PION BEAMS

Stanley B. Curtis

January 1970

AEC Contract No. W-7405-eng-48

LAWRENCE RADIATION LABORATORY
UNIVERSITY of CALIFORNIA BERKELEY

48

DISCLAIMER

HUMAN KIDNEY CELL OXYGEN-ENHANCEMENT RATIOS FOR FAST-NEUTRON BEAMS AND A PREDICTION FOR NEGATIVE PION BEAMS[1]

Stanley B. Curtis

Lawrence Radiation Laboratory
University of California
Berkeley, California 94720

[1]Work supported by the U. S. Atomic Energy Commission.

No. of copies submitted 3
Manuscript pages 26
No. of figures 11
No. of tables 4

Curtis, Stanley B., Human Kidney Cell Oxygen-Enhancement Ratios for Fast-Neutron Beams and a Prediction for Negative Pion Beams. Radiation Res.___ pp.____ - ____(1970).

ABSTRACT

A semiphenomenological theory is developed to estimate survival curves of human kidney (T-1) cells in vitro from irradiation by particle beams that produce broad LET distributions. "Track segment" data are used where appropriate, and heavy recoils ($Z > 2$) are treated separately. The assumption is made that such recoils inside the cell nucleus inactivate and those outside do not. The calculated oxygen-enhancement ratios from 3- and 15-MeV monoenergetic neutron beams compare favorably with experimental results; thus the constancy of this ratio as a function of neutron energy is quantitatively understood. The survival curves, however, agree less well with experiment, perhaps due to inadequate assumptions made for the inactivation cross sections of low energy protons, for which no experimental data are available. The oxygen-enhancement ratio in the peak dose region of a stopping π^- beam is calculated to be between 1.8 and 2.0, slightly higher than the values obtained for the neutron beams. It is concluded that the α-particle component is very important in the 15-MeV neutron and stopping pion beams, both in producing inactivation and in depressing the oxygen-enhancement ratio.

****

KEY WORDS: Oxygen enhancement ratio, fast neutrons, π^- beams, cellular inactivation, human kidney cells.

INTRODUCTION

In the extensive experiments by Barendsen and his colleagues, in which survival of human kidney cells (T-1) in vitro was measured after irradiation in both the oxygenated and anoxic state with various beams of fast neutrons, it was found that the oxygen-enhancement ratio (OER) is close to 1.6 for beams of quite widely distributed energies (fission spectrum up to 15 MeV monoenergetic) (1-3). That OER is not dependent on neutron energy is puzzling at first glance, since the LET distributions as calculated by Bewley (4) vary significantly for beams of different energies. Also, it might be expected that the OER would rise as a function of neutron energy, since the average LET_∞ of the recoil proton decreases at higher neutron energies. The lack of variation can be explained qualitatively by the assumption that the higher-LET components (from α particles and heavy recoils) play a particularly prominent role in the biological damage process [as has already been suggested by Broerse et al. (3) and Bewley (5)].

In this paper we investigate this suggestion quantitatively by developing a semiphenomenological theory of cell survival, using data from "track segment" experiments by Barendsen et al. (1) where applicable (i.e., for the LET_∞ range up to 2500 MeV cm^2/g, which includes the proton and α-particle components), and by treating the heavy nuclear recoils separately. A similar study by Bewley (5), using a different approach to the survival calculation, resulted in only moderate success at reproducing the experimental values of OER. In addition, if the OER values for neutrons thus calculated are close

to the experimental values, a similar calculation for π^- should yield an OER close to the one that would be measured if pion beams of adequate intensity were available.

The interest in π^- beams stems from their possible suitability for use in tumor radiotherapy. They possess a combination of properties not shared by other radiation modalities: favorable depth-dose characteristics, a high-LET contribution in the peak-dose region, and a predominance of low-LET components elsewhere (6-10). Since many tumors are known to contain hypoxic cells, it is of interest to determine the extent to which pion radiation can overcome the oxygen effect.

FORM OF THE SURVIVAL EXPRESSION

The first step in the development of such a semiphenomenological theory is to select a consistent method of calculating survival curves. A study by Todd (11) of the proliferative capacity of human kidney cells (T-1) in vitro irradiated with heavy ions with single-valued LET_∞ at the Berkeley Hilac has shown that the survival curves can be adequately described by an analytical expression of the form

$$S = \exp(-D/D_1)\,\{1-[1-\exp(-D/D_2)]^n\}, \qquad (1)$$

where D is the dose in rads and D_1, D_2, and n are constants for an ion with a given LET_∞. The constants D_1 and D_2 can be related to the probabilities for a damaging event to occur in a cell per incident particle fluence. The dose D is proportional to the product of the fluence (N) and the LET_∞ (L) of the particles. The exponents in equation 1 may also be written as the product $N\sigma$, where σ is the inactivation probability per incident particle fluence. Equating $N\sigma_1$

to D/D_1 and $N\sigma_2$ to D/D_2 and properly including the proportionality constant, we obtain

$$\sigma_1 = 1.6L/D_1 \quad \text{and} \quad \sigma_2 = 1.6L/D_2,$$

where L is the LET_∞ (or dE/dx) in MeV cm^2/g, D_1 and D_2 are in rads, and the cross sections, σ_1 and σ_2, are in μ^2. The σ_1 cross section has been interpreted as being associated with single-hit single-target damage and σ_2 has been associated with multitarget damage. We may now write the survival expression in general form,

$$S(D) = \exp[-\eta(D, \sigma_1)] \langle 1 - \{1 - \exp[-\eta(D, \sigma_2)]\}^n \rangle, \tag{2}$$

where, in the case of single-valued LET_∞ radiation, the exponents are

$$\begin{aligned} \eta(D, \sigma_1) &= \frac{D}{1.6} \frac{\sigma_1}{L}, \\ \eta(D, \sigma_2) &= \frac{D}{1.6} \frac{\sigma_2}{L}. \end{aligned} \tag{3}$$

THE EMPIRICAL FORM OF INACTIVATION CROSS SECTIONS

Barendsen's "track segment" data, obtained with deuterons and α particles (1) for the same cell system and biological end point as Todd, have been analyzed, and it is found that the identical expression adequately describes the survival curves in these experiments. The data and the calculated curves are shown in Fig. 1. Here n in equation 2 was set equal to 6, an average value measured by Todd.[2] The curves were calculated by using cross-section values obtained from

2. P. W. Todd, Reversible and irreversible effects of ionizing radiations on the reproductive integrity of mammalian cells cultured in vitro, UCRL-11614 (1964) Ph. D. thesis.

analytical expressions as a function of LET_∞ constructed so as to adequately fit the data (see Appendix I for the expressions used). Figure 2 shows the dependence on LET_∞ for the four cross sections, σ_1 and σ_2 for the oxygenated and for the anoxic cases. Todd's data from the high-energy heavy ions are shown as experimental points for the oxygenated (aerobic) case. At low LET_∞, where the same particles are used (deuterons and α particles), the agreement between Barendsen's and Todd's results is good. At higher LET_∞, where Todd used heavier ions all at the same velocity and Barendsen used α particles at lower energies, the agreement is not so good. This lack of agreement is probably an example of the breakdown of LET_∞ as a universal parameter for specifying biological effect, as is to be discussed in a subsequent paper.

GENERALIZATION OF THE SURVIVAL EXPRESSION TO ACCOMMODATE RADIATIONS WITH LET DISTRIBUTIONS

The absorbed dose produced by neutron and pion beams is composed of contributions from the various charged particles (protons, α particles, and heavy recoils) resulting from the nuclear interactions that the particles undergo in the medium. LET spectra for the various neutron beams used by Barendsen have been calculated by Bewley (4) and a similar spectrum has been calculated for stopping pions (10).

For particles having a range of energies characterized by differential energy spectra, dN/dE, at the dose point, we have, for the exponents in equation 2,

$$\eta(D, \sigma) = \int \left[\sum_i \frac{dN_i}{dE} \sigma(E) \right] dE, \tag{4}$$

where the summation is over the particle types having energy E. In the neutron case, for example, we have three terms,

$$\eta(D, \sigma) = \int \left[\frac{dN_p}{dE} \sigma(E) + \frac{dN_\alpha}{dE} \sigma(E) + \frac{dN_R}{dE} \sigma(E) \right] dE,$$

where p, α, and R denote protons, α particles, and heavy recoils, respectively. Expressing equation 4 as an integral over LET_∞ instead of over the energy, we have

$$\eta(D, \sigma) = \int_{L_{min}}^{L_{max}} \left[\sum_i \frac{dN_i}{dE} \sigma(L) \left(\frac{dE}{dL}\right)_i \right] dL, \tag{5}$$

where L_{min} and L_{max} are the minimum and maximum LET_∞ produced by the radiation, and $\sigma(L)$ is assumed to be a universal function of L over the region of integration.

Now we define the LET distribution F(L) so that

$$\int F(L)dL = \text{Dose} = D \int F_N(L)dL, \tag{6}$$

where $F_N(L)$ is the normalized LET distribution: $\int F_N(L)dL = 1$. Since the dose can also be defined

$$\text{Dose} = \int \left[\sum_i \frac{dN_i}{dE} L_i \right] dE = \int \left[\sum_i \frac{dN_i}{dE} L_i \left(\frac{dE}{dL}\right)_i \right] dL, \tag{7}$$

we can equate integrands in equation 6 and 7, obtaining

$$F(L) = \sum_i \frac{dN_i}{dE} L_i \left(\frac{dE}{dL}\right)_i = L \sum_i \frac{dN_i}{dE} \left(\frac{dE}{dL}\right)_i .$$

We then substitute $\frac{F(L)}{L}$ for $\sum_i \frac{dN_i}{dE} \left(\frac{dE}{dL}\right)_i$ in equation 5, obtaining

$$\eta(D, \sigma) = \int_{L_{min}}^{L_{max}} F(L) \frac{\sigma(L)}{L} dL = D \int_{L_{min}}^{L_{max}} F_N(L) \frac{\sigma(L)}{L} dL.$$

Equations 3 then become, for a broad LET distribution,

$$\eta(D, \sigma_1) = \frac{D}{1.6} \int_{L_{min}}^{L_{max}} F_N(L) \frac{\sigma_1(L)}{L} dL,$$

$$\eta(D, \sigma_2) = \frac{D}{1.6} \int_{L_{min}}^{L_{max}} F_N(L) \frac{\sigma_2(L)}{L} dL, \qquad (8)$$

where D is the number of rads, $F_N(L)$ is the normalized LET distribution, L is the LET_∞ in MeV cm^2/g, and σ is in μ^2. We have assumed that each element of dose acts independently via either of two inactivation mechanisms characterized by inactivation cross sections σ_1 and σ_2.

SEPARATE TREATMENT OF THE HEAVY RECOILS

Above an LET_∞ of 2500 MeV cm^2/g, only the very-low-energy heavy recoils are present, and there are no experimental data on inactivation cross sections for them. The only available data in this range are the high-energy heavy-ion data of Todd's, and they are

plotted as data points and as short dashed lines at high LET_∞ in Fig. 2.

Because it is possible that cross sections obtained at high velocity are not relevant to lower-velocity ions of the same LET_∞, the heavy recoils were treated separately. It was assumed that a heavy recoil ($Z > 2$) inactivated the cell if it traveled through the cell nucleus, and failed to inactivate if it traveled only in the cytoplasm. That is, the inactivation probability was assumed to be unity for a recoil inside the cell nucleus and zero outside. In addition, it was assumed that this probability is oxygen-independent, i.e., identical for the oxygenated and anoxic states. Thus, the exponent $\eta(D, \sigma_1)$ was modified by setting $L_{max} = 2500$ and by adding an additional term to include the heavy recoils,

$$D \rho_R (V_S + V_C) \quad \text{recoil inactivations/cell,}$$

where ρ_R = number of recoils/cm^3 rad,

V_S = sensitive volume in cm^3 (assumed to be the volume of the cell nucleus),

V_C = the additional effective volume due to recoils arising in the cytoplasm and penetrating the cell nucleus.

The resulting expression for $\eta(D, \sigma_1)$ becomes

$$\eta(D, \sigma_1) = \frac{D}{1.6} \int_{L_{min}}^{2500} F_N(L) \frac{\sigma_1(L)}{L} \, dL + D\rho_R(V_S + V_C). \qquad (9)$$

The second exponent, $\eta(D, \sigma_2)$, was changed only by setting $L_{max} = 2500$; it was assumed that damage from heavy recoils was of the single-hit single-target type and that inactivation depended only on whether a

recoil was inside the cell nucleus.

NEUTRON SURVIVAL CURVES

A computer program was developed for the CDC 6600 which calculates survival curves for a given LET distribution for both the anoxic and oxygenated cases, using the analytical expressions for the cross sections given in Appendix I and the survival expressions given by equations 2, 8, and 9. Two neutron beams of energy 3 and 15 MeV were chosen. Monoenergetic beams were selected so that ρ_R could be readily calculated. This quantity is obtained from the expression

$$\rho_R = \frac{N_0 \rho}{M\phi} \sum_{i=1}^{3} (N_i \sigma_{Ri}) \qquad \text{heavy recoils/cm}^3 \text{ rad},$$

where N_0 = Avogadro's number,

ρ = density of tissue (assumed to be 1 g/cm^3 here),

M = molecular weight of tissue (assumed to be 402 from the approximation $C_5H_{40}O_{18}N$),

ϕ = fluence-to-dose conversion factor [in rads/(neutron/cm^2)],

N_i = number of atoms of the ith element per molecule of tissue,

σ_{Ri} = neutron-recoil reaction cross section for the ith element (in cm^2).

Values of σ_{Ri}, ϕ, and ρ_R for the two neutron energies are given in Table I. All recoil production mechanisms, both elastic and inelastic, were included.

For the neutron irradiations, the recoils can be assumed to arise solely from within the nucleus of the cell, since the maximum range of

a recoil is around 2μ for the 15-MeV neutrons and is even less for the 3-MeV neutrons,[3] and the cell nucleus is assumed to have a diameter of 8μ. V_s is calculated assuming a sphere of radius 4μ. Therefore, we have $V_s = 268\ \mu^3$ and $V_c = 0$ for the neutron cases.

The calculated curves and experimental data, along with the corresponding LET distribution from Bewley (4), are shown for the 3-MeV and 15 MeV neutron beams in Fig. 3. Again n was set equal to 6. The dashed lines at high dose indicate the results obtained using Todd's data at high LET_∞ instead of treating the heavy recoils separately.

OXYGEN ENHANCEMENT RATIOS

In this paper, the calculated oxygen enhancement ratio (OER) is defined as the ratio of the dose leading to a given survival of cells in the anoxic state to the dose leading to the same survival of cells in the oxygenated state. Therefore, OER depends on the survival level chosen. From the computed survival curves in Fig. 1, the OER's for the "track segment" data can be calculated. Figure 4 presents the ranges (indicated by pairs of arrows) of calculated OER from 0.3 to 0.01 survival at the LET_∞ values investigated by Barendsen et al. (1), along with their experimental values. The agreement is good, as expected, since the survival curves were calculated with parameters chosen so that the curves would fit the experimental data.

3. J. J. Broerse, Effects of energy dissipation by monoenergetic neutrons in mammalian cells and tissues (Thesis). Publication of the Radiobiological Institute TNO of the Organization of Health Research TNO, Rijswijk, The Netherlands, 1966.

COMPARISON OF NEUTRON OER's

The OER's for the 3-MeV and 15-MeV neutron beams from the survival curves shown in Fig. 3 are presented along with the measured values in Fig. 5. Here the hatched areas indicate the calculated range of OER over all survival levels down to 0.01. The agreement is quite good, and is considerably better than the agreement between calculated and experimental survival curves shown in Fig. 3. Thus, the survival-curve calculation is a more sensitive test of the adequacy of the theoretical treatment than the OER comparison. On the other hand, it appears that OER can be predicted adequately even with the theory in its present crude form.

OER PREDICTION FOR NEGATIVE PIONS IN THE REGION OF THE AUGMENTED BRAGG PEAK

By use of the theoretical LET distribution (10) calculated from experimental data in water-impregnated nuclear emulsion (9), the survival curves can be calculated for a hypothetical exposure from a π^- beam in the peak region of the augmented Bragg curve. The procedure for treating the recoils in this case is given in Appendix II. We note here that the range distribution of recoils from pion stars is broad enough so that a significant contribution to the inactivation arises from recoils which are produced in the cytoplasm and which subsequently penetrate into the cell nucleus. The increase in effective volume is 344 μ^3, thus making the total effective sensitive volume 612 μ^3 for pions, compared with 268 μ^3 for neutrons. The calculated curves are shown along with the LET distribution in Fig. 6. No claim is made for the absolute accuracy of the individual survival curves. In fact, the

deviation from experiment is expected to be comparable to that observed for neutrons. It is reasonable to assume, however, that the OER predicted will be close to that which would be measured. The predicted OER's for the "pure" and contaminated beams are shown in Fig. 5. They fall in the range 1.8 to 2.0, slightly higher than for the neutron beams. The incident pion beam in this calculation had a Gaussian momentum distribution, 190 ± 5 MeV/c, and the peak of the augmented Bragg curve occurred at 25.5 cm of water (10). The contaminated incident beam consisted of 10% muons and 25% electrons, an experimental situation at the Berkeley 184-inch synchrocyclotron. (8).

A summary of calculated OER's for the neutron and π^- beams, plus a comparable calculation by Bewley (5), all at 1% survival level, and the published experimental results with neutron beams (3), are presented in Table II.

LOW-DOSE LIMITING VALUES

Although the experimental survival curves for the neutron irradiations drop more precipitously with increasing dose than do the calculated curves (as seen in Fig. 3), inspection of the very-low-dose region reveals that the initial slopes of the curves are in considerably better agreement. Since only $\eta(D, \sigma_1)$ is important at low doses, we can neglect the second factor is equation 2 and assume a simple exponential curve given by $\exp[-\eta(D, \sigma_1)]$. In particular, it is of interest to investigate the quantity $\eta(D, \sigma_1)/D$, which is the probability of inactivation per cell per rad. This is also the reciprocal of the initial D_{37},

and is measure of the initial slope of the survival curve. The contributions to this quantity from the various components of the beams are also of interest. Table III presents the total probabilities of cell inactivation per rad and the contributions from different particles present in the beams. The effective sensitive nuclear volume is also shown for neutrons and pions. The initial OER is obtained simply as the ratio of the probability of cell inactivation for the oxygenated cells to that for the anoxic cells. These are given in the last column of the table as the low-dose limiting values.

The percentage contributions to cell inactivation from the various particles composing the beams are presented in Table IV along with their percentage contributions to the absorbed dose for comparison. It is interesting to note the importance of the α-particle contribution to cell inactivation by 15-MeV neutrons.

In contrast, the recoil contribution is less for 15-MeV neutrons than for 3-MeV neutrons. It appears that it is the α-particle contribution at higher neutron energy that keeps the OER low. In pion irradiation the α particles play an even more significant role, contributing between 40 and 50% of the cell inactivation, while contributing less than 15% of the dose.

THE VARIATION OF OER WITH DEPTH THROUGH THE BRAGG PEAK OF A PION BEAM

It is interesting from the radiotherapeutic standpoint to estimate how the OER might vary through the peak region of a beam of stopping

π^-. A beam design has been studied by Thiessen[4] in connection with the "meson factory" now being constructed at Los Alamos Scientific Laboratory. The characteristics of the incident beam were chosen so that the peak dose would span a 10-cm region centered at 15 cm depth of water. The incident energy spectrum of the beam is shown in Fig. 7, and is assumed to be "pure pions." The LET distributions at various depths have been calculated in the same manner as in the previous work (10), and are given in Fig. 8. They show a slow increase in the importance of the high-LET portions as the depth of water increases. At 9 cm of water no stars are present and the distribution is due only to pions which have not yet stopped. As more of the pions stop in going through the region, the distribution favors the higher-LET components. The integrals of these distributions are proportional to the doses at the various depths. The depth-dose curve for this beam is shown in Fig. 9. Also shown is the variation of OER through the peak region as calculated by the phenomenological theory described above. It drops sharply from around 3.0 to 2.2 as the region is entered, and then decreases to 1.8 at the end of the stopping region for this beam. The variation depends strongly on the shape of the incident energy spectrum, and other variations can be produced by other energy spectra. The lower limit of OER from this theoretical treatment is 1.54, calculated for "star" radiation only, with no contribution from pions still moving. Finally, the lowest curve is Fig. 9 shows the variation in density of pion stars through the peak dose region.

4. H. A. Thiessen, A design study of a π^- beam for biomedical applications at LAMPF, Los Alamos Report LA-DC-9789, 1968.

DISCUSSION

This attempt, first to understand T-1 cell survival curves resulting from neutron irradiation, and second to make a prediction for pion irradiation, using data from "track segment" experiments, is hampered mainly by the lack of experimental data on inactivation cross sections for low-energy protons. It is clear from Fig. 3 that the use of high-energy heavy-ion data in the high-LET range results in an inadequate description of the survival curves. The volumetric treatment of the recoils appears to give results closer to experiment, though the fit of the theoretical and experimental curves could certainly be improved. The cross sections for protons in the LET_∞ region between 600 and 900 MeV cm^2/g were assumed to be the same as for deuterons and α particles in the same region of LET_∞. This assumption may not be valid, and adjustments of the cross sections in this region may have to be made. The necessity for such adjustments for different particles at the same LET_∞ would be another example of the inadequacy of LET_∞ for uniquely specifying biological damage, as suggested by Rossi (12) in general and by Bewley in this specific case (5). The lack of validity may be particularly important for the 3-MeV neutron beam, where the α particle data were used up to an LET_∞ of 1000 MeV cm^2/g, even though no α particles are present in the beam. It may be, however, that this effect influences the oxygenated and anoxic cases to a similar extent, so that in the ratio of doses required for the OER calculation, the error is not so large as in the survival-curve calculation itself. The agreement between the theoretical and experimental values of OER for 3-MeV neutrons is reassuring in this regard.

Other assumptions that affect the results are the size of the radio-sensitive volume of the T-1 cell and the appropriate values of the neutron-nucleus recoil cross sections. Different assumptions made by Bewley (5) for these quantities, plus the different approach to the calculation of the survival curves, probably account for the differences between his results and those reported here.

The importance to inactivation of the α-particle contribution in the 15-MeV neutron beam is clearly seen in Table IV. The results for the pion beams also indicate the importance of this component. Thus, the specific conclusion can be drawn that the α-particle component dominates the inactivation in both the 15-MeV neutron and pion irradiations and is a more important factor than even the heavy recoils in depressing the OER for both these irradiations.

SUMMARY

A semiphenomenological theory has been developed to try to understand the experimental neutron survival curves and OER's obtained with T-1 human kidney cells, by utilizing "track segment" data where available and by treating the recoils separately. In addition, a prediction of OER for the peak region of a π^- beam has been made. The following conclusions are drawn from this analysis:

1. It is possible to describe the "track segment" survival curves in terms of two inactivation cross sections by the analytical expression

$$S(L, D) = \exp\frac{[-D\sigma_1(L)]}{1.6\,L} \left\{1 - \left[1 - \exp\frac{[-D\sigma_2(L)]}{1.6\,L}\right]^n\right\},$$

where D is the dose in rads, $\sigma_1(L)$ and $\sigma_2(L)$ are the inactivation cross sections in μ^2 (given in Appendix I), L is the LET_∞ in MeV cm^2/g, and n, the "extrapolation number," is set equal to 6.

2. By using a generalization of the survival expression to accommodate an LET distribution and an empirically determined dependence of cross section on LET_∞ up to 2500 MeV cm^2/g, and by treating the heavy recoils separately, the oxygen enhancement ratios are adequately predicted for the 3-MeV and 15-MeV neutron beams. If high-energy heavy-ion results are assumed at high LET, poorer agreement with the experimental results is obtained.

3. Agreement between experimental and theoretical OER's is better than the agreement of the individual survival curves, suggesting that the effect causing the lack of survival-curve agreement cancels out in the OER calculation. One suggestion for the discrepancy is that proton inactivation cross sections may not be adequately approximated by the deuteron and α-particle "track segment" data. The results at low dose, where the survival can be considered exponential, are probably more precise than at higher doses, where multiple events from the low-LET components play a more significant role in the inactivation.

4. The α-particle component at high neutron energy is crucial in keeping the OER low, and is also very important in the inactivation and low OER expected for pion beams.

5. The OER predicted for the augmented Bragg peak of a π^- beam, calculated in the same way as for neutrons, is in the range 1.8 to 2.0, slightly higher than the neutron values. For a beam with a broad pion energy spectrum, the OER drops sharply as the peak dose region is

entered and then decreases slowly through the region. For a beam with peak dose region 10 cm broad, centered at 15 cm of water, the OER varied from 2.2 to 1.8 through the region. Although the absolute magnitude of the OER may be somewhat imprecise due to the nature of the assumptions that must enter the theoretical considerations, the theory should provide an accurate trend of the variation and a rough estimation of the degree to which the oxygen effect will be overcome by π^- irradiation.

ACKNOWLEDGMENTS

The author wishes to acknowledge discussions with Drs. J. F. Fowler and G. W. Barendsen concerning an early version of this paper. Dr. V. P. Bond suggested the calculation of the variation of OER through the peak-dose region of the π^- beam. The suggestions of Drs. M. R. Raju and H. A. Thiessen are also gratefully acknowledged. The interest, support and encouragement of Profs. C. Richman, C. A. Tobias and J. H. Lawrence are greatly appreciated.

APPENDIXES

I. Analytic expressions for σ_1 and σ_2.

The expressions used for σ_1 and σ_2 below an LET_∞ of 2500 MeV cm^2/g are as follows:

$$\sigma_1 = 35\,[1 - \exp(-\alpha_1 L - \beta_1 L^2 - \gamma_1 L^3 - \delta_1 L^8)]\,\mu^2$$

$$\sigma_2 = 25\,[1 - \exp(-\alpha_2 L - \beta_2 L^2)] \text{ for } \sigma_2 \leq 15\ \mu^2$$

$$= 15 \text{ when the above expression } > 15\ \mu^2.$$

For the oxygenated case:

$$\alpha_1 = 9 \times 10^{-5},$$

$$\alpha_2 = 3 \times 10^{-4},$$

$$\beta_1 = 3 \times 10^{-7},$$

$$\beta_2 = 5 \times 10^{-7},$$

$$\gamma_1 = 6 \times 10^{-10},$$

$$\delta_1 = 2.3 \times 10^{-25}.$$

For the anoxic case:

$$\alpha_1 = 2 \times 10^{-5},$$

$$\alpha_2 = 1.2 \times 10^{-4},$$

$$\beta_1 = 2 \times 10^{-7},$$

$$\beta_2 = 3.5 \times 10^{-7},$$

$$\gamma_1 = 1 \times 10^{-10},$$

$$\delta_1 = 3 \times 10^{-25}.$$

II. Calculation of probability of inactivation from recoils in π^- beams.

We calculate first the number of recoils/cm^3 rad, ρ_R, and then the additional effective volume (V_c) due to recoils originating in the cytoplasm and penetrating the cell nucleus. The inactivation probability per rad from recoils can then be obtained for pions as shown in Table III from the expression $\rho_R(V_s + V_c)$, with $V_s = 268\ \mu^3$ as before.

The number of recoils/cm^3 rad is given by

$$\rho_R = N_R \rho_I / \phi,$$

where N_R = probability of a recoil per pion interaction,

ρ_I = density of pion interactions per incidence fluence [in number per (cm^3 - incident pion/cm^2)],

= density of stopping pions per incidence fluence, since every stopping pion is captured and interacts,

ϕ = fluence-to-dose conversion factor (in rads per incident pion/cm^2).

The value of N_R is given by

$$N_R = \sum_i P_i N_i A_i / \sum_i N_i A_i,$$

where P_i = probability of a recoil's being produced in a pion capture by the ith element.

N_i = number of atoms of the ith element per molecule of tissue,

A_i = atomic weight of the ith element.

The P_i's come from the experimental work of Fowler and Mayes (9). The N_i's come from the approximation formula of tissue ($C_5H_{40}O_{18}N$) and the A_i's reflect the assumption that the capture probability in a compound varies as the atomic weight. The calculated value of N_R is

0.737 recoil per pion interaction. Both the ϕ and ρ_I values vary with incident energy spectrum and depth of absorber. The values applying to the beams with incident Gaussian momentum spectra of 190 ± 5 MeV/c are: ρ_I = 0.1711 pion interactions/[cm^3(incident pion/cm^2)], and $\phi = 1.514 \times 10^{-7}$ rads/(incident pion/cm^2) for the contaminated beam peak at 25.5 cm of water (25% electrons and 10% muons in the incident beam) and $\phi = 1.274 \times 10^{-7}$ rads/(incident pion/cm^2) for the pure pion beam peak.

For the calculation of V_c, we determine the number of recoils intersecting a cell nucleus from outside, assuming a constant density of pion interactions and isotropic emission of recoils. We write the expression for the number of intersections (i.e., inactivations) per(cell × incident fluence)

$$N_c = \int \rho_N P(r_1)\, dV = N_R \rho_I V_c,$$

where ρ_N = number of recoils per(unit volume × incident fluence) = $N_R \rho_I$,

$P(r_1)$ = probability of inactivation per recoil event at a distance r_1 from the surface of the cell nucleus.

So we have for the "effective" sensitive volume in the cytoplasm, V_c, the expression

$$V_c = \int P(r_1) dV.$$

Now dV for this symmetrical problem is given by

$$dV = 4\pi(r_1 + R)^2\, dr_1,$$

where R = the radius of the cell nucleus (see Fig. 10). Therefore, we have

$$V_c = 4\pi \int_0^\infty (r_1 + R)^2 P(r_1) dr_1. \qquad (1A)$$

We now calculate $P(r_1)$, the probability that, given a recoil at a distance r_1 from the surface of a sphere of radius $R(=4\mu$ here), the recoil will penetrate the surface. Referring to Fig. 10, we have, from the Law of Cosines,

$$r^2 + (r_1 + R)^2 - 2r(r_1 + R)\cos\theta = R^2.$$

Solving this quadratic equation for r and taking the negative sign in the solution (the positive sign would require the recoil to traverse the nucleus completely), we obtain

$$r = (r_1 + R)\cos\theta - [(r_1+R)^2 \cos^2\theta - 2r_1R - r_1^2]^{1/2}. \qquad (2A)$$

From the work of Fowler and Mayes (9), we have the recoil integral range distribution produced by pion captures in oxygen, which we can normalize to unity at zero range (actually 1μ was used, since shorter recoils could not be observed). This gives the probability $P_R(>r)$ that a recoil will travel at least a distance r in "wet emulsion." This dependence is shown in Fig. 11. Although "wet emulsion" has a density of 2.0, the greater stopping power of water when expressed in MeV cm^2/g, probably cancels much of this effect. Thus, it was decided to use the integral range distribution in "wet emulsion" directly as an approximation to the integral range distribution in tissue. This assumption is, if anything, on the conservative side, and the recoil ranges are perhaps slightly underestimated. An additional assumption was made that the recoil range distributions from the other elements

in tissue do not differ significantly from the one measured for oxygen. The other two important heavy elements in tissue--carbon and nitrogen--are close to oxygen in the periodic table, and thus might be expected to produce similar recoil range distributions. The experimental data to substantiate this assumption, however, are lacking at present.

We now calculate the fractional solid angle subtended by the sphere at a given r_1, weighted by the probability that the recoil goes at least a distance r,

$$P(r_1) = \frac{1}{4\pi} \int_0^{\Omega_{max}} P_R(>r) d\Omega = \frac{1}{2} \int_0^{\theta_{max}} P_R(>r) \sin\theta \, d\theta, \quad (3A)$$

where $P_R(>r)$ is read from Fig. 11. The value of r is a function of r_1 and θ, and is calculated for given r_1 and θ from equation 2A. The value of θ_{max} is easily seen from Fig. 10 to be

$$\theta_{max} = \sin^{-1}\left[\frac{R}{r_1 + R}\right].$$

The integrations in equation 3A were performed numerically for various values of r_1, and finally V_c was calculated by numerically integrating equation 1A from a plot of $(r_1 + R)^2 P(r_1)$ as a function of r_1. The result is 344 μ^3. When added to the 268-μ^3 nuclear volume, this more than doubles the sensitive cell volume for inactivation from recoils produced in stopping π^- beams for cells with nuclei 8 μ in diameter.

REFERENCES

1. G. W. Barendsen, C. J. Koot, G. R. van Kersen, D. K. Bewley, S. B. Field, and C. J. Parnell, The effect of oxygen on impairment of the proliferative capacity of human cells in culture by ionizing radiations of different LET. Intern. J. Radiation Biol. 10, 317-327 (1966).
2. G. W. Barendsen and J. J. Broerse, Dependence of the oxygen effect on the energy of fast neutrons. Nature 212, 722-724 (1966).
3. J. J. Broerse, G. W. Barendsen, and G. R. van Kersen, Survival of cultured human cells after irradiation with fast neutrons of different energies in hypoxic and oxygenated conditions. Intern. J. Radiation Biol. 13, 559-572 (1968).
4. D. K. Bewley, Calculated LET distributions of fast neutrons. Radiation Res. 34, 437-445 (1968).
5. D. K. Bewley, A comparison of the response of mammalian cells to fast neutrons and charged particle beams. Radiation Res. 34, 446-458 (1968).
6. P. H. Fowler and D. H. Perkins, The possibility of therapeutic applications of beams of negative pi mesons. Nature 189, 524-528 (1961).
7. P. H. Fowler, Pi-mesons versus cancer? Proc. Phys. Soc. (London) 85, 1051-1066 (1965).
8. C. Richman, H. Aceto, M. R. Raju, and B. Schwartz, The radiotherapeutic possibilities of negative pions-preliminary physical experiments. Am. J. Roentgenol. Radium Therapy Nucl. Med. 96, 777-790 (1966).

9. P. H. Fowler and V. M. Mayes, The capture of pi-mesons in oxygen and in other nuclei. Proc. Phys. Soc. (London) 92, 377-389 (1967).

10. S. B. Curtis and M. R. Raju, A Calculation of the physical characteristics of negative pion beams-energy loss distribution and Bragg curves. Radiation Res. 34, 239-255 (1968).

11. P. W. Todd, Reversible effects of densely ionizing radiation upon the reproductive capacity of cultured human cells. Med. College Virginia Quarterly 1[4], 2-14 (1966).

12. H. H. Rossi, Correlation of radiation quality and biological effect. Ann. N. Y. Acad. Sci. 114, 4-15 (1964).

FIGURE CAPTIONS

Fig. 1. "Track segment" survival curves (oxygenated and anoxic) for human kidney cells in vitro, obtained at the various LET_∞ values indicated. The data are Barendsen's experimental data (1), and the solid curves are calculated as explained in the text.

Fig. 2. Inactivation cross sections, σ_1 and σ_2, for the oxygenated and anoxic irradiations. The data points are heavy-ion data (11). The curves are analytical expressions given in Appendix I, constructed to fit Barendsen's α-particle and deuteron data (1).

Fig. 3. The calculated (solid line) and experimental survival curves and LET spectra (4) for 3-MeV and 15-MeV neutron beams (oxygenated and anoxic irradiations). The dashed lines at high doses show the curves obtained using the Todd data at high LET_∞. The experimental data for 3-MeV neutrons were obtained at a low dose rate of $\approx$ 1 rad/min.

Fig. 4. The oxygen enhancement ratios (OER) as a function of LET_∞ for the "track segment" experiments. The experimental points are Barendsen's (1), and the arrows indicate the range of calculated OER for survival levels 0.3 to 0.01.

Fig. 5. The oxygen enhancement ratios (OER) for neutrons at two energies. The experimental points are from Broerse et al. (2, 3), and the hatched areas indicate the range of calculated OER down to 0.01 survival. The OER for π^- beams ("pure" and contaminated) are also shown as calculated for beams with incident Gaussian momentum spectra 190 ± 5 MeV/c.

Fig. 6. The calculated survival curves (oxygenated and anoxic irradiations) and LET spectrum (10) for the peak region of "pure" and contaminated π^- beams with incident momentum spectra 190 ± 5 MeV/c.

Fig. 7. Incident pion differential energy spectrum producing a broad peak (10 cm wide) centered at 15 cm depth of water (from Thiessen).

Fig. 8. The LET distributions at various depths produced by the pion beam with energy spectrum of Fig. 7. The depths increase from bottom to top of this graph.

Fig. 9. The variation of OER, dose, and density of stopping pions as a function of depth through a water absorber for the beam with incident energy spectrum shown in Fig. 7.

Fig. 10. Geometry of a recoil event occurring at a distance r_1 from the surface of sphere of radius R. The recoil travels at an angle θ to the line joining event and sphere center.

Fig. 11. Normalized integral range distribution of recoils from pion capture by oxygen in "wet emulsion" [from Fowler and Mayes(9)].

PHYSICAL QUANTITIES FOR THE SEPARATE TREATMENT OF RECOILS IN THE NEUTRON SURVIVAL CURVE CALCULATIONS

Beam Energy	Cross section (cm^2)			Fluence-to-Dose Conversion Factor $\left[\frac{rads}{(neutron/cm^2)}\right]$	ρ_R $\left[\frac{No.\ of\ recoils}{cm^3 \cdot rad}\right]$
	Carbon	Nitrogen	Oxygen		
3 MeV	2.2×10^{-24} [a]	1.7×10^{-24} [a]	1.6×10^{-24} [a]	3.62×10^{-9} [d]	1.72×10^{7}
15 MeV	1.12×10^{-24} [b]	1.6×10^{-24} [b]	1.59×10^{-24} [c]	6.73×10^{-9} [d]	7.97×10^{6}

a. C.K. Bockelman, D.W. Miller, R.K. Adair and H.H. Barschall, Total cross sections of light nuclei for p,T-neutrons. Phys. Rev. 84, 69-75 (1951) There is a resonance in carbon and an intermediate value was chosen .

b. M.L. Randolph, Energy deposition in tissue and similar materials by 14.1-MeV neutrons. Rad. Res. 7, 47-57 (1957)

c. R.C. Axtmann and J.A. Licari, Yield of the Fricke dosimeter to 14.6-MeV neutrons. Rad. Res. 22, 511-518 (1964)

d. R.L. Bach and R.S. Caswell, Energy transfer to matter by neutrons. Rad. Res 35, 1-25 (1968)

DBL 6912 5199

Table I

OXYGEN ENHANCEMENT RATIOS AT 1% SURVIVAL

	Present Work	*Todd Approximation at High dE/dx*	*Bewley*[a]	*Experiment*[b]
3-MeV Neutrons	1.57	1.90	1.80	1.5±0.3
15-MeV Neutrons	1.57	1.70	1.74	1.6±0.2
Contaminated Pions (10% Muons, 25% Electrons)	1.98	1.89	—	—
"Pure" Pions	1.90	1.81	—	—

a. From Bewley (4). Table IV. line 3 (Barendsen's track segment data, with CNO interactions considered separately) was used for comparison.

b. Best value considering the whole survival curve.

DBL 701 5540

Table II

CALCULATED LOW DOSE INACTIVATION PARAMETERS

Particle Beam	Cell Environment	Effective Sensitive Volume for Recoils (cm^3)	Probability of Cell Inactivation/rad				Initial D_{37} (rads)	Low Dose OER
			From recoils	From Alphas	From Other Particles	Total		
3 MeV Neutrons	Oxygenated	2.68×10^{-10}	4.61×10^{-3}	———	5.68×10^{-3}	10.29×10^{-3}	97	1.47
	Anoxic	"	"	———	2.37×10^{-3}	6.98×10^{-3}	143	
15 MeV Neutrons	Oxygenated	"	2.14×10^{-3}	2.52×10^{-3}	2.41×10^{-3}	7.07×10^{-3}	141	
	Anoxic	"	"	1.94×10^{-3}	0.84×10^{-3}	4.92×10^{-3}	203	1.44
Pions * (25% e^- 10% μ^-)	Oxygenated	6.12×10^{-10}	0.51×10^{-3}	1.47×10^{-3}	1.8×10^{-3}	3.78×10^{-3}	265	1.86
	Anoxic	"	"	1.03×10^{-3}	0.49×10^{-3}	2.03×10^{-3}	493	
Pions * (Pure)	Oxygenated	"	0.61×10^{-3}	1.75×10^{-3}	1.76×10^{-3}	4.12×10^{-3}	243	1.76
	Anoxic	"	"	1.23×10^{-3}	0.5×10^{-3}	2.34×10^{-3}	428	

* *At the Bragg peak of a pion beam with initial Gaussian momentum distributions: 190 ± 5 MeV/c.*

DBL 6912 5200

Table III

PERCENTAGE CONTRIBUTION TO INACTIVATION AND DOSE FROM DIFFERENT PARTICLES

Particle Beam	Cell Environment	Percent Cell Inactivations Per Rad			Percent Dose Deposited		
		By Protons	By Alpha Particles	By Heavy Recoils	By Protons	By Alpha Particles	By Heavy Recoils
					From BEWLEY (4)		
3-MeV Neutrons	Oxygenated	55	—	45	92	—	8
	Anoxic	34	—	66			
15-MeV Neutrons	Oxygenated	34	36	30	71	18	11
	Anoxic	17	39	44			
		By All Particles Except Alphas & Recoils			By All Particles Except Alphas & Recoils		
					From CURTIS & RAJU (10)		
Pions (25% e^- 10% μ^-)	Oxygenated	48	39	13	78	12	10
	Anoxic	24	51	25			
Pions (Pure)	Oxygenated	43	42	15	75	14	11
	Anoxic	21	53	26			

DBL 6912 5201

Table IV

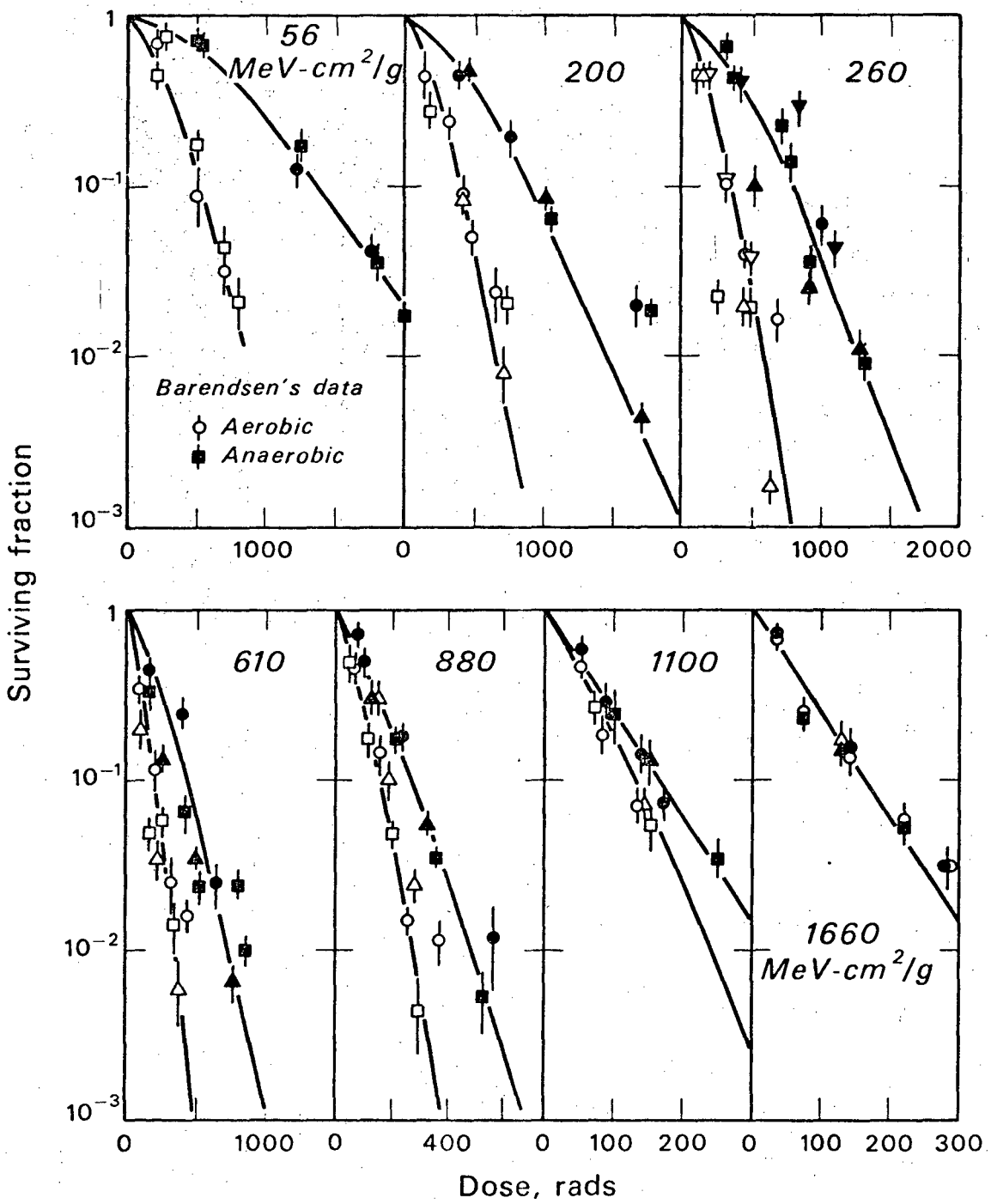

DBL 681-4527

Fig. 1

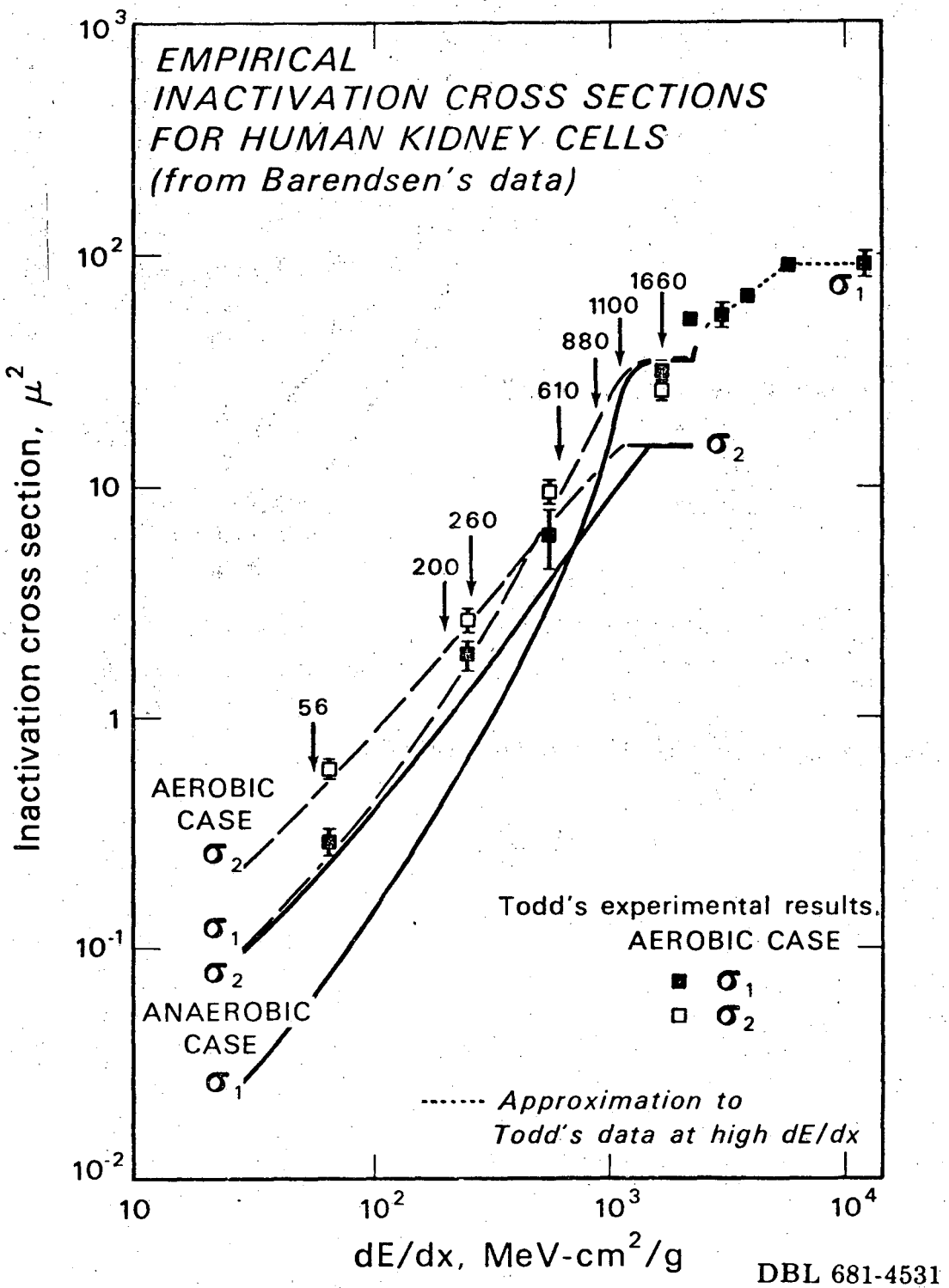
EMPIRICAL
INACTIVATION CROSS SECTIONS
FOR HUMAN KIDNEY CELLS
(from Barendsen's data)
Inactivation cross section, μ^2
dE/dx, MeV-cm^2/g
10^3
10^2
10
1
10^{-1}
10^{-2}
10
10^2
10^3
10^4
56
200
260
610
880
1100
1660
σ_1
σ_2
AEROBIC CASE
σ_2
σ_1
σ_2
ANAEROBIC CASE
σ_1
Todd's experimental results,
AEROBIC CASE
σ_1
σ_2
Approximation to
Todd's data at high dE/dx
DBL 681-4531

Fig. 2

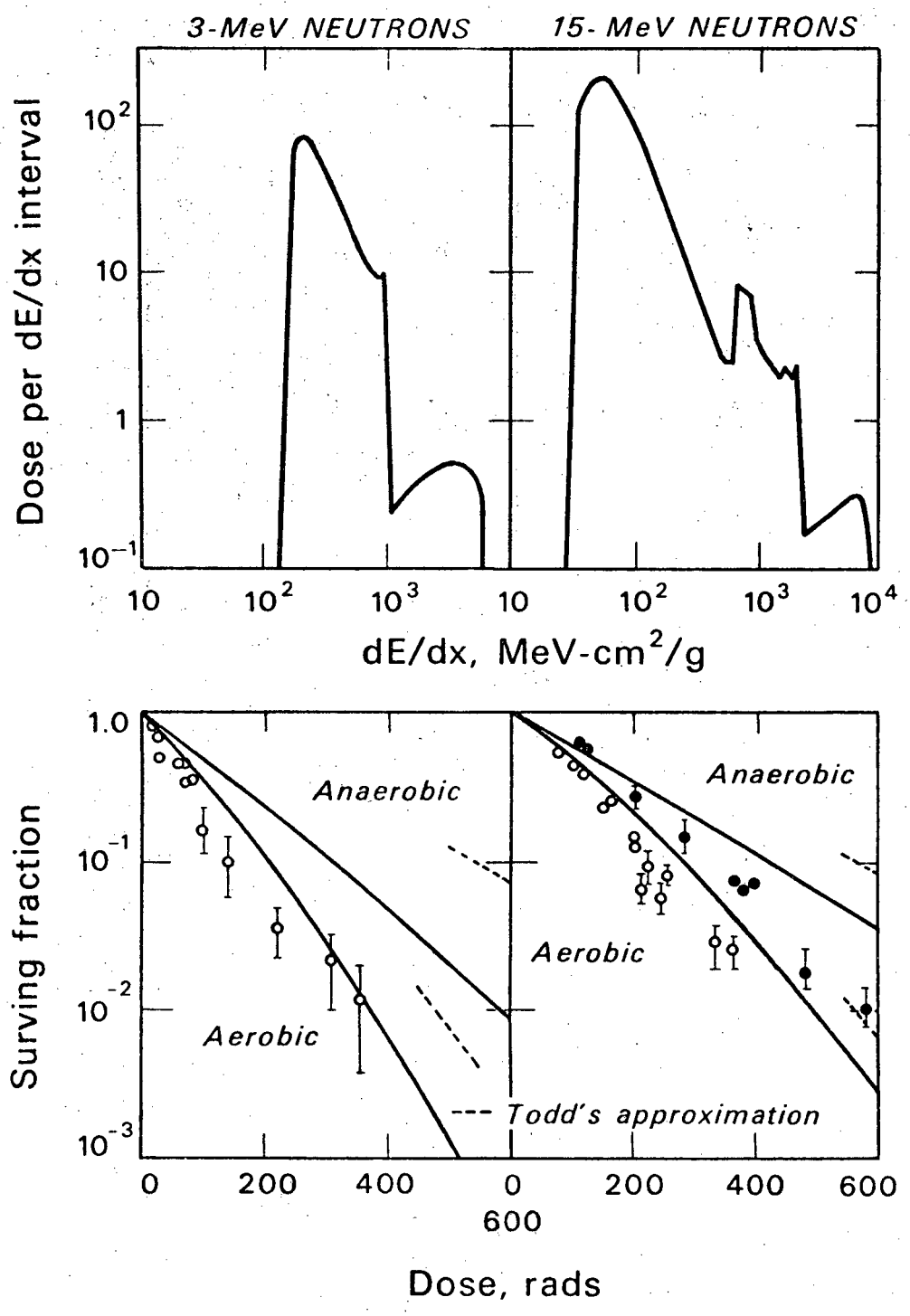

DBL 701 5539

Fig. 3

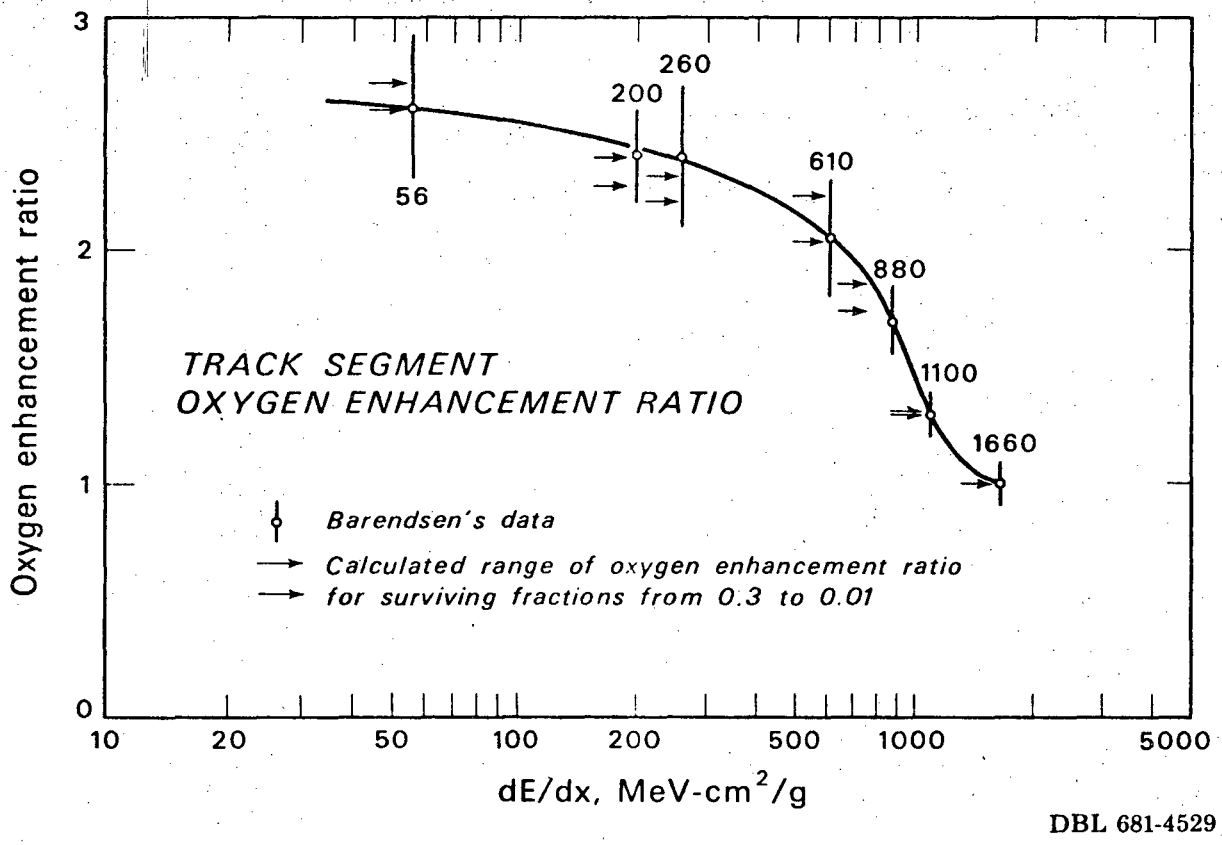
Oxygen enhancement ratio
3
2
1
0
10
20
50
100
200
500
1000
5000
dE/dx, MeV-cm²/g
56
200
260
610
880
1100
1660
TRACK SEGMENT
OXYGEN ENHANCEMENT RATIO
Barendsen's data
Calculated range of oxygen enhancement ratio
for surviving fractions from 0.3 to 0.01
DBL 681-4529

Fig. 4

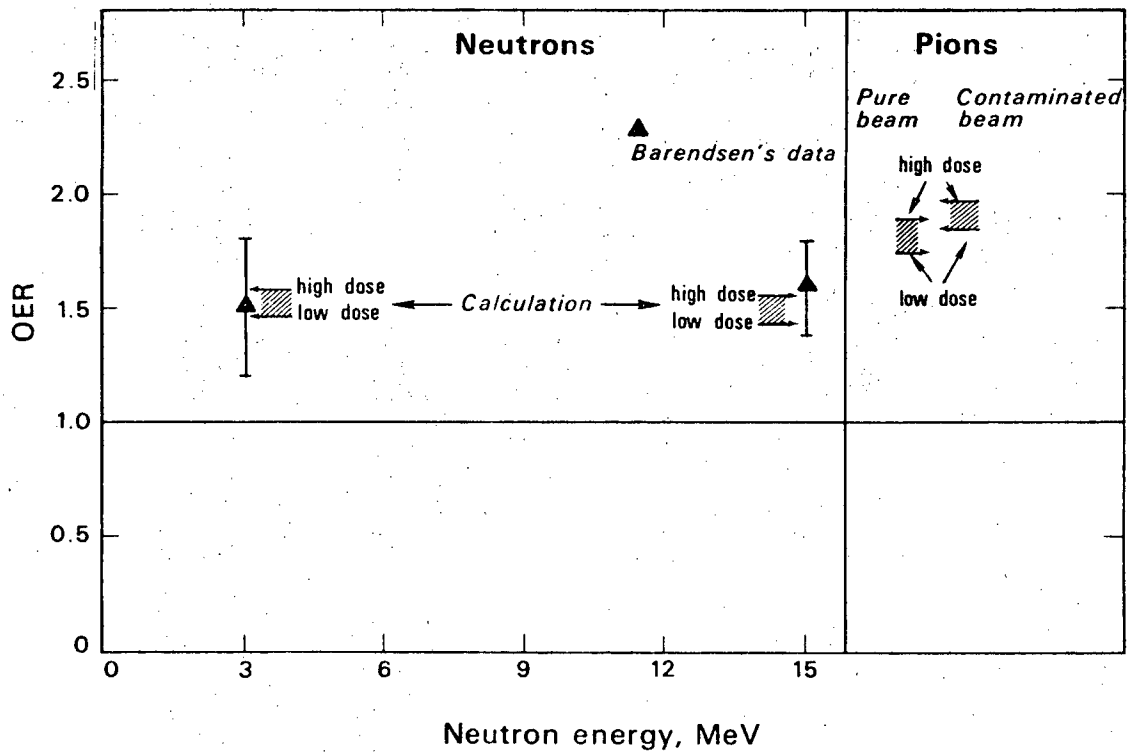

DBL 6912 5197

Fig. 5

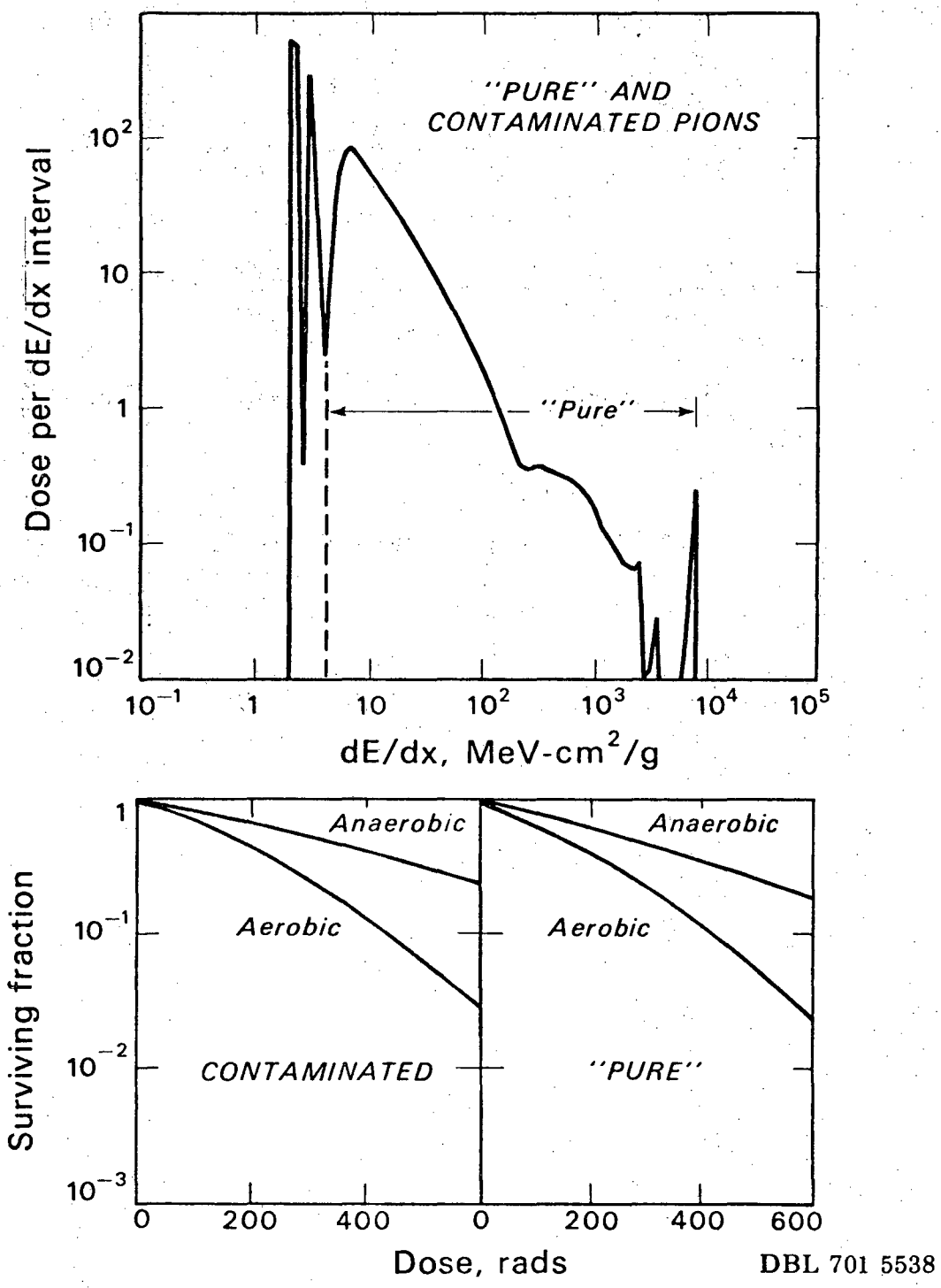
"PURE" AND
CONTAMINATED PIONS
"Pure"
Dose per dE/dx interval
dE/dx, MeV-cm²/g
Anaerobic
Aerobic
CONTAMINATED
Anaerobic
Aerobic
"PURE"
Surviving fraction
Dose, rads
DBL 701 5538

Fig. 6

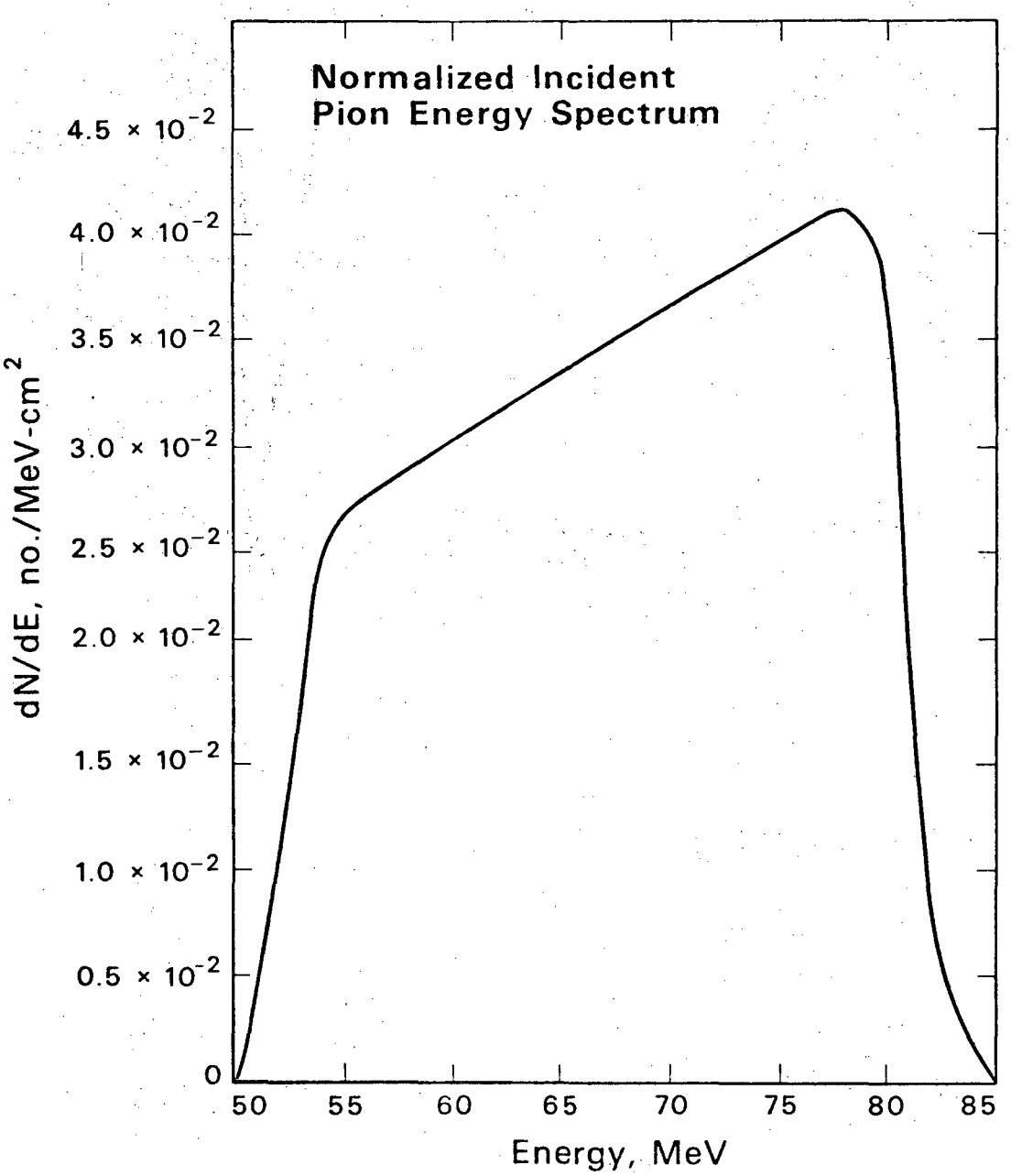

DBL 6912 5198

Fig. 7

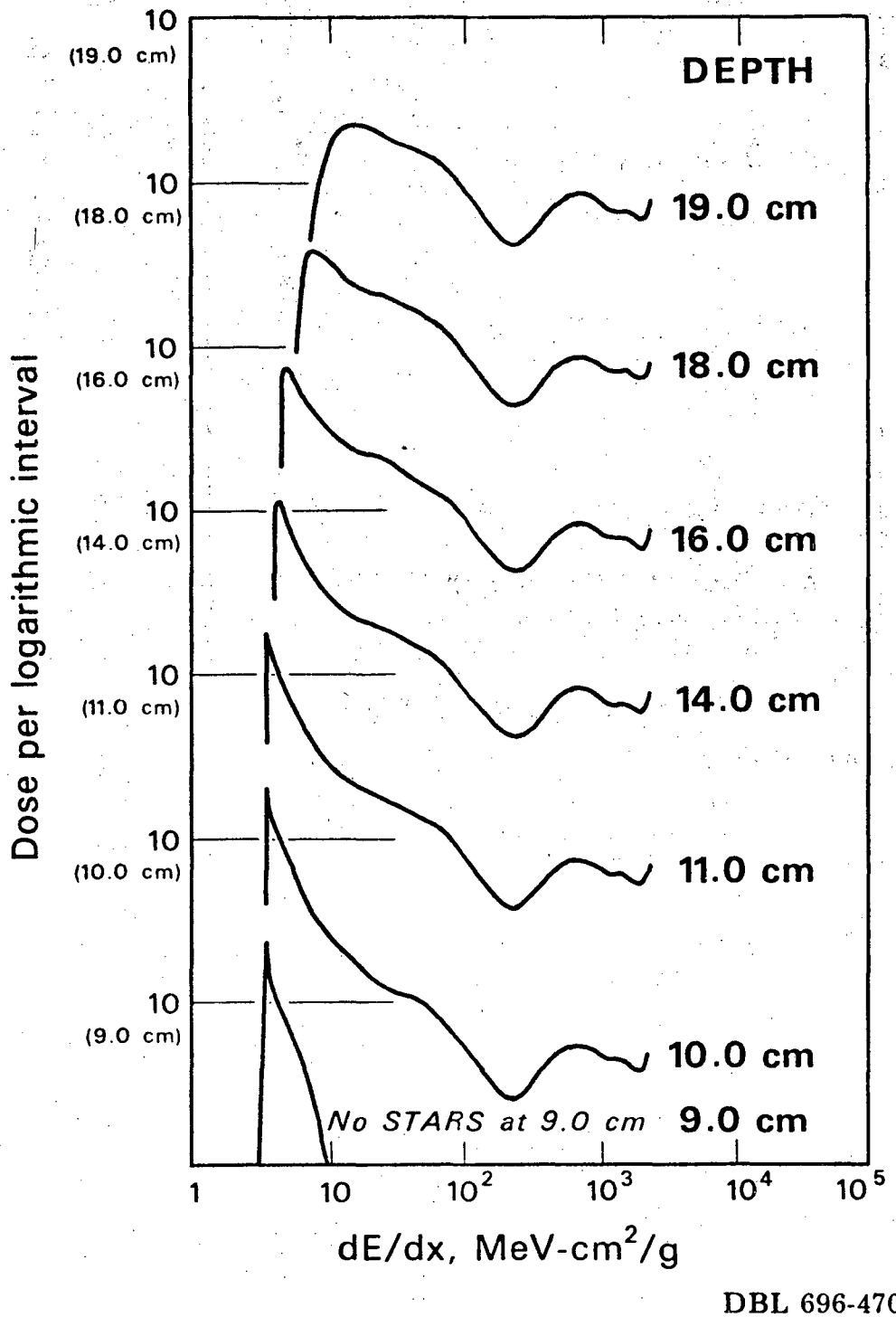

DBL 696-4702

Fig. 8

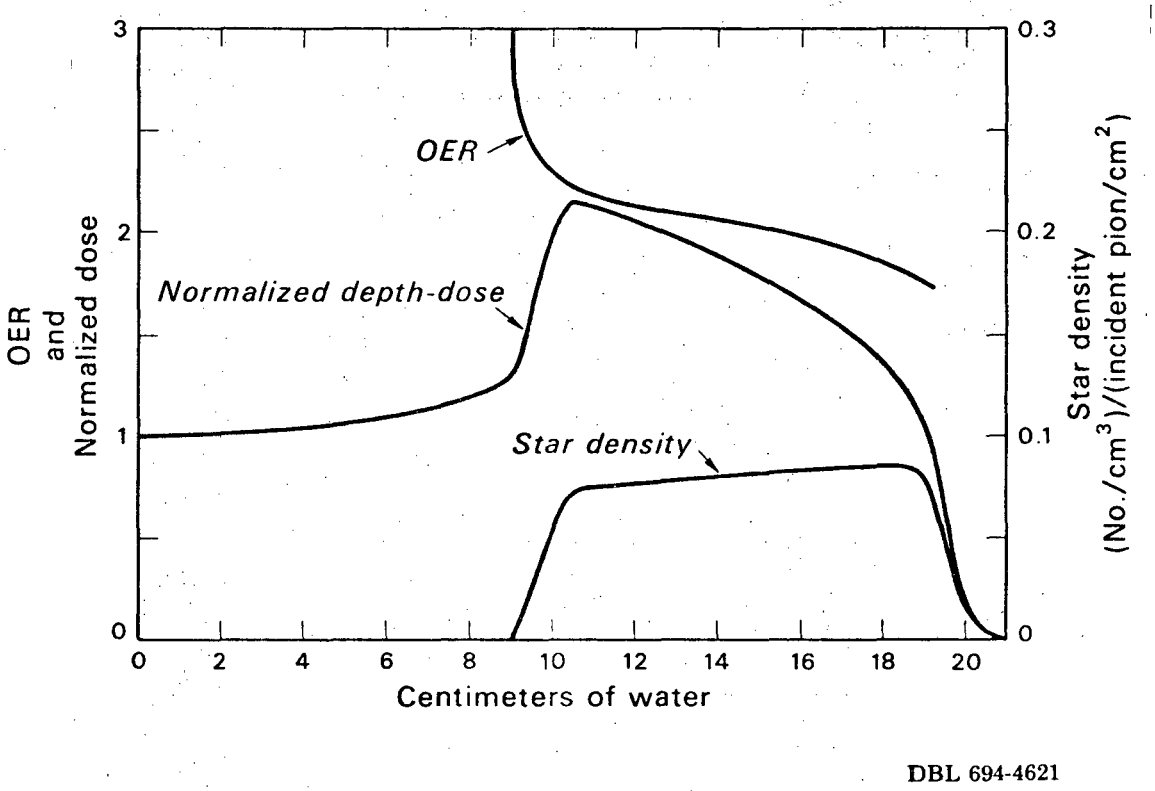
OER
Normalized depth-dose
Star density
OER and Normalized dose
Star density (No./cm³)/(incident pion/cm²)
Centimeters of water
0
1
2
3
0.1
0.2
0.3
0
2
4
6
8
10
12
14
16
18
20
DBL 694-4621

Fig. 9

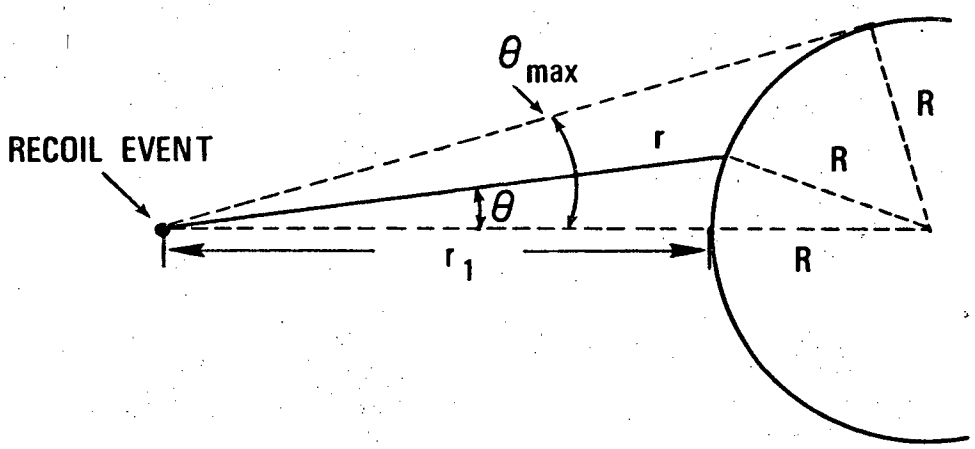

Fig. 10

DBL 701 5541

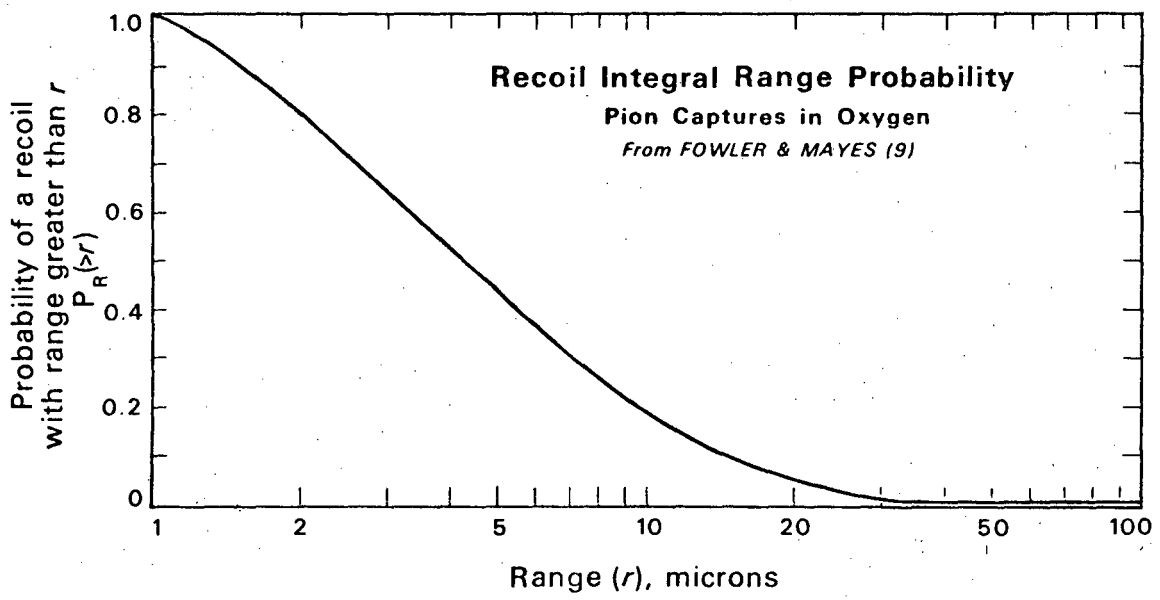

DBL 701 5542

Fig. 11

TECHNICAL INFORMATION DIVISION
LAWRENCE RADIATION LABORATORY
UNIVERSITY OF CALIFORNIA
BERKELEY, CALIFORNIA 94720